Meteoroid Engineering Model (MEM) 3: NASA's newest meteoroid model

Althea V. Moorhead[(1)]

[(1)]NASA Meteoroid Environment Office, Marshall Space Flight Center EV44,
Huntsville, Alabama, USA, althea.moorhead@nasa.gov

ABSTRACT

Meteoroid impacts threaten spacecraft and astronauts at all locations within the Solar System. At certain altitudes in low-Earth orbit, orbital debris dominates the risk, but meteoroids are more significant within 250 km of the Earth's surface and above 4000 km [1]. In interplanetary space, orbital debris is nonexistent and meteoroids constitute the entire population of potentially dangerous impactors. The NASA Meteoroid Environment Office (MEO) produces the Meteoroid Engineering Model (MEM) to support meteoroid impact risk assessments [2]; MEM is a stand-alone piece of software that describes the flux, speed, directionality, and bulk density of meteoroids striking a spacecraft on a user-supplied trajectory. The MEO released version 3 of MEM in 2019 [3]. This proceeding describes the orbital populations that form the core of MEM, highlights key differences between MEM 3 and its predecessors, discusses the implications of these changes for spacecraft, summarizes our validation against meteor and in-situ data, and delineates the model's limitations.

1 INTRODUCTION

MEM's purpose is to enable spacecraft designers to assess the probability of meteoroid impacts, predict the resulting damage to spacecraft components, and, if necessary, add the appropriate amount of shielding. However, MEM itself provides only a description of the meteoroid environment and does not predict the number of craters or penetrations. The damage done by a meteoroid impact depends on the spacecraft's materials and shape, and is described by damage equations or ballistic limit equations (BLEs). For example, the following equation is known as the modified Cour-Palais BLE [4] and gives the depth of an impact crater, p_c:

$$p_c \propto d^{19/18}\, \rho^{1/2}\, \left(v_\perp \cos\theta\right)^{2/3} \tag{1}$$

where d, ρ, v, and θ are the diameter, density, speed, and impact angle of a projectile. Thus, MEM must provide not just the rate of impacts, but also the speeds, densities, and direction of motion of meteoroids.

Furthermore, MEM must be able to describe the meteoroid flux at various locations in the Solar System, despite the fact that nearly all meteoroid measurements are obtained in near-Earth space. Thus, a physics-based approach is needed in order to extrapolate from the near-Earth environment to the Moon, planets, and interplanetary space. MEM satisfies these needs by combining a physics-based model of meteoroid orbits [5], a physics-based model of the meteoroid mass distribution [6], and recent meteoroid density measurements [7, 8]. In essence, MEM consists of a set of meteoroid orbits and corresponding physical parameters. Meteoroids are overwhelmingly produced by comets – specifically, short-period comets, Halley-type comets, and long-period comets. These comets have large orbits, with aphelia near Jupiter or far beyond; thus, while the meteoroid environment varies over interplanetary distances, the Earth and Moon encounter essentially the same population of meteoroids.

The core orbital populations within MEM are based on [5]. In brief, [5] simulated the production of meteoroids from four populations of parent bodies: short-period comets, long-period comets, Halley-type comets, and asteroids. [5] then modeled the evolution of these orbits under the influence of radiative forces (such as Poynting-Robertson drag, [9, 10]) and mutual collisions. The resulting populations were then compared with observed features of the meteor complex; the helion and antihelion sources appeared to originate from short-period comets, the apex sources from long-period comets, and the toroidal sources from Halley-type comets. No observed feature matches the asteroidal population generated by [5], and we have therefore excluded it from MEM 3 entirely [3]. These so-called "sources" refer to concentrations of meteor radiants within a Sun-centered ecliptic reference frame, and are labeled in Fig. 1, which presents the directionality of the meteoroid environment as seen from a 1 au orbit.

One useful feature of the meteoroid environment is that is does not vary over short distances. While the flux at Mars differs from that at the Earth, the Earth-Moon distance is insignificant in comparison with meteoroid dynamical

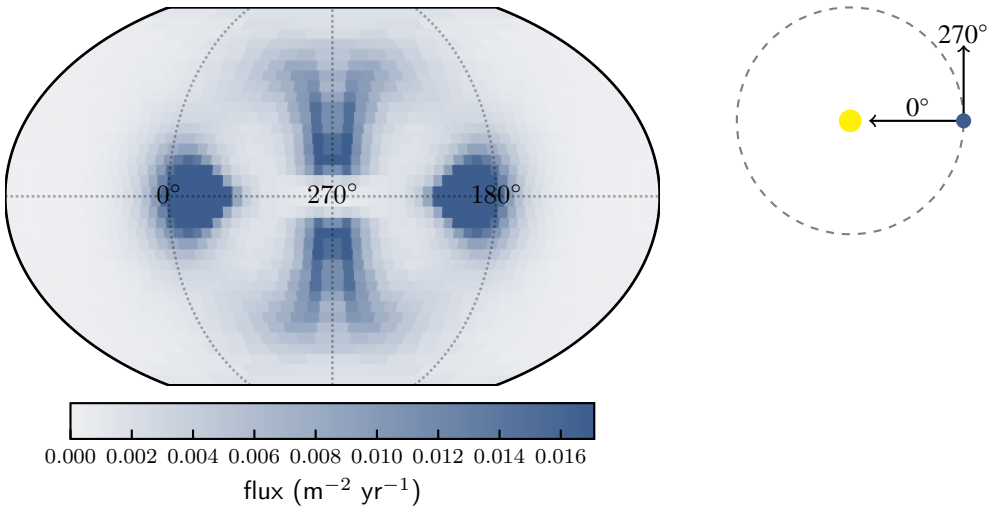

Fig. 1: Map of meteoroid directionality (left) relative to a spacecraft traveling around the Sun on a 1-au orbit, outside the Earth's sphere of influence. The color reflects the flux per angular bin, and the coordinate system is a non-inertial one in which an azimuthal angle of 270° points in the direction of the spacecraft's motion around the Sun (right).

length scales. Thus, the Earth and the Moon can be considered to encounter the same population of meteoroids. The gravity and physical size of the Earth and Moon do, however, locally modify their environment in a way that is mathematically predictable (see Section 2.1). MEM 3 automatically determines whether the user's spacecraft passes near a massive body and takes these effects into account.

MEM does not output a generic meteoroid environment description. Instead, it reports the flux, speed distribution, directional distribution, and bulk density distribution of meteoroids encountered along a specific spacecraft trajectory, which must be provided by the user. The spacecraft's velocity and, to a limited extent, its orientation are incorporated into the outputs.

2 CORRECTIONS AND IMPROVEMENTS

Prior to releasing MEM 3, the Meteoroid Environment Office conducted an in-depth review of the existing code base and completely refactored the code to produce software that is more accurate, more efficient, and more robust. Frequent regression testing was used to minimize the chances of introducing new errors, and new tests, such as the Öpik test described in Section 2.1, were implemented to ensure that the new code functioned as desired. This process uncovered a number of errors in the existing code base that were repaired in MEM 3. Several desired new features – such as a more detailed density distribution – were also incorporated into the model. In this section, we describe four of the most significant differences between MEMR2 and MEM 3; a comprehensive list of all changes is provided in ref. [3].

2.1 Gravitational focusing and planetary shielding

Most spacecraft orbit a massive body such as the Earth, Moon, or other planet. The meteoroid environment near such a body will differ from that in interplanetary space; gravity will alter the trajectory of meteoroids that pass nearby, and a large object will also physically block some meteoroids from reaching the spacecraft [11–13]. The first effect can cause local enhancements of the meteoroid flux that we call "gravitational focusing," and the latter effect we refer to as "planetary shielding."

These effects are illustrated in the leftmost panel of Fig. 2 for a monodirectional flow of meteoroids. Meteoroids (white lines) approach from the left and their trajectories bend in response to the planet's gravity and are in some cases ended where the planet blocks their path. The background color reflects the corresponding local number density

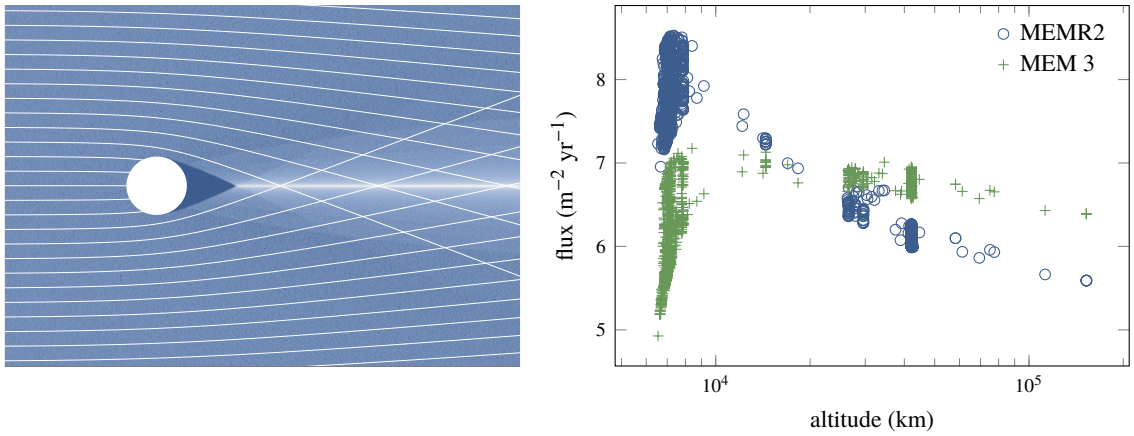

Fig. 2: Illustration of the effects of gravitational focusing and shielding (left) and the resulting variation of flux with altitude (right). The plot at right presents the flux of meteoroids larger than 10^{-6} g calculated by MEMR2 and MEM 3 for a number of randomly selected spacecraft in low Earth orbit.

of the meteoroids; dark blue areas are less densely populated and light blue areas are more densely populated. Areas with enhanced number density and flux occur where meteoroid trajectories overlap.

Gravitational focusing and planetary shielding vary depending on the relative placement of the meteoroid radiant, gravitational body, and spacecraft; MEM uses the equations of [12] to calculate the effect on the meteoroid flux, directionality, and speed for the spacecraft's given location. However, when averaged over a sphere of constant altitude, conservation of energy ensures that gravitational focusing obeys a fairly simple relation:

$$\frac{\text{flux}_1}{\text{flux}_2} = \left(\frac{\text{speed}_1}{\text{speed}_2}\right)^2 \tag{2}$$

where flux_1 and speed_1 are the meteoroid flux and speed at one altitude, and flux_2 and speed_2 are the meteoroid flux and speed at another altitude. We applied this relationship to MEM – called the Öpik test – as a test of its gravitational focusing routine. This test revealed that the gravitational focusing in MEMR2 was exaggerated; this has been repaired in MEM 3.

The corrected gravitational focusing algorithm produces fluxes in LEO that are more similar to those encountered at higher altitudes. To illustrate the difference, we have converted a large number of spacecraft two-line element sets (TLEs) to state vectors and used them as inputs to both MEMR2 and MEM 3. The total meteoroid flux computed by each model for these spacecraft is presented in the rightmost panel of Fig. 2. Note that MEM 3 predicts a lower (mass-limited) meteoroid flux for spacecraft in low Earth orbit (LEO) and a higher flux for spacecraft that are more distant from the Earth.

2.2 Correlations between direction and speed

A meteoroid's speed is correlated with its radiant; for instance, apex meteoroids can impact the Earth with speeds as large as 72 km s^{-1}, while antapex meteoroids cannot exceed 12 km s^{-1}. This is because the heliocentric escape velocity at 1 au is about 42 km s^{-1} and the Earth's orbital velocity is about 30 km s^{-1}. As a result, retrograde, nearly parabolic comets can intercept the Earth "head-on" at speeds approaching 72 km s^{-1}. In contrast, prograde comets intercept the "wake" or "aft" side of the Earth at speeds of only 12 km s^{-1}. These two cases serve as an example of how the speed of a meteoroid and its directionality relative to the Earth (or spacecraft) are correlated. Figure 3 displays a heat map of the average meteoroid speed per directional bin at 1 au according to MEMR2 (left) and MEM 3 (right).

The correlation between meteoroid direction and speed is much less pronounced in MEMR2 then it is in MEM 3. An in-depth review of the code revealed that MEMR2 erases any correlations between direction and speed within each sporadic population. MEMR2 erroneously assumed that the meteoroid radiant-speed distribution could be obtained

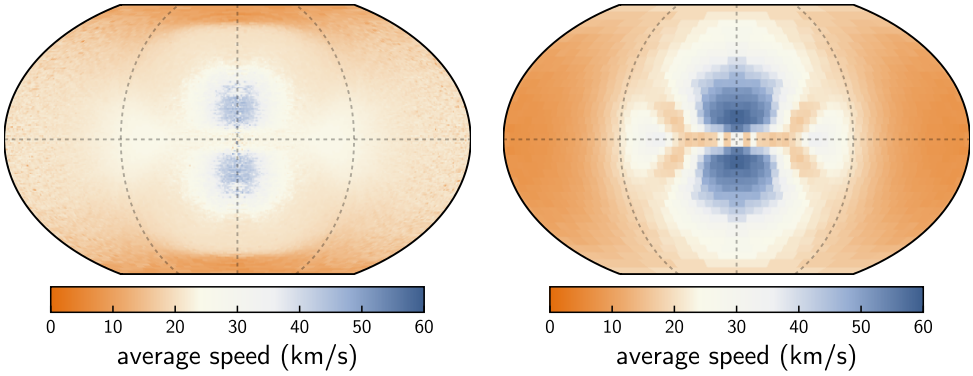

Fig. 3: Average speed per directional bin at 1 au in Sun-centered ecliptic coordinates as modeled by MEMR2 (left) and MEM 3 (right).

by multiplying the radiant distribution by the speed distribution for each source. As a result, the few correlations that remained were simply due to variations in the directional distribution of the sporadic sources. MEM 3 removes this assumption and computes and stores the meteoroid flux within a three-dimensional grid that covers all possible combinations of radiant and speed.

For the same meteoroid mass, a higher speed translates to a higher kinetic energy and usually a deeper impact crater or penetration depth. It is therefore critical to accurately reproduce these correlations in order to predict which sides of a spacecraft will experience high-speed impacts. Spacecraft designers may wish to concentrate their shielding on surfaces that experience higher speed impacts, for instance.

2.3 Sporadic source strengths

Using both MEMR2 and MEM 3, we simulated the meteoroid flux incident at the top of the atmosphere and extracted the fraction of that flux produced by each meteoroid orbital population (or sporadic source). We then compared these fractions with the de-biased relative source strengths measured by [14] and [15]. In MEMR2, the modeled toroidal source is significantly stronger than observed, and the helion and apex sources are weaker than observed. The source strengths in MEM 3 have been adjusted to provide a better match to the data (see the left panel of Fig. 4).

Each source is tied to a distinct orbital population and thus also has a distinct speed distribution. As modeled by [5], the toroidal population are, on average, the slowest, while the apex population is the fastest. When we reduce the strength of the toroidal population and increase the strength of the helion and apex populations to better match observations, the overall speed distribution shifts to faster speeds. This is apparent in the right panel Fig. 4, which shows the meteoroid speed distribution at the top of the atmosphere calculated by MEMR2 and MEM 3.

The meteoroid speed distribution will vary with the spacecraft's position and velocity, but the speed distribution generated by MEM 3 will be faster than that produced by MEMR2 in most, if not all, cases. Both damage and attitude disturbances will increase with meteoroid speed, and thus this change to the speed distribution will lead to higher risk estimates overall.

2.4 Bulk density distribution

All previous versions of MEM assumed a constant meteoroid bulk density of 1 g cm^{-3}. This was based on the state of knowledge at the time: meteoroids originate primarily from comets and thus are likely to consist primarily of ice, which has a density of about 0.9 g cm^{-3}. This assumption was supported by an attempt to measure meteoroid densities using ALTAIR radar measurements of their decelerations in the atmosphere [16].

These initial density measurements were somewhat crude and the radar meteor data set they used skewed strongly toward apex meteoroids. Ref. [7] later revisited the problem of meteoroid densities with a more sophisticated meteor ablation model and cutting edge optical meteor measurements. They found that meteoroid densities appeared to be correlated with Tisserand parameter, a quantity used to classify orbits as cometary or asteroidal in nature. Meteoroids

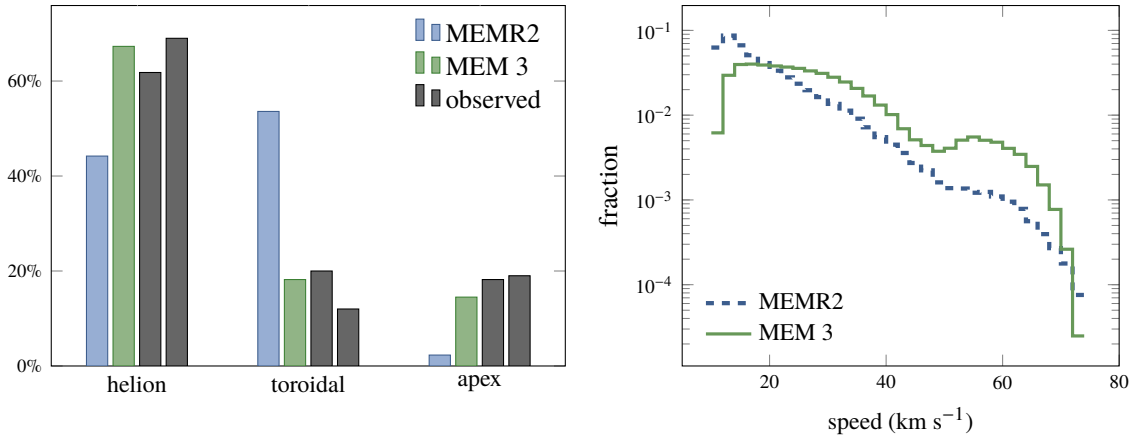

Fig. 4: Left: relative strength of the sporadic sources at the top of the Earth's atmosphere as modeled by MEMR2 and MEM 3 and as observed by refs. [14] and [15]. Right: Speed distribution of meteoroids entering the Earth's atmosphere as calculated by MEMR2 and MEM 3.

on shorter orbits, like those of asteroids and Jupiter-family comets, had higher densities while those with longer orbits had lower densities.

The correlation between meteoroid density and orbital classification uncovered by ref. [7] allows us to construct a meteoroid density distribution for MEM. We fit two log-normal distributions to the density measurements obtained by ref. [7]. We then assigned the low-density distribution to the apex and toroidal orbital populations, which have longer orbital periods, and the high-density distribution to the helion and antihelion population, which are produced by short-period comets [8]. Figure 5 presents the resulting density distribution of meteoroids at the top of the Earth's atmosphere as modeled by MEM 3 and compares it with the single value assumed by MEMR2.

For a given meteoroid mass, a higher density corresponds to deeper, wider craters and penetration of thicker surfaces. The new high-density population in MEM 3 will therefore tend to increase damage estimates.

3 MODEL VALIDATION

We have tested MEM 3 in numerous phases of its development. As mentioned in Section 2, we first conducted an in-depth review and complete refactoring of the code base that included repeated regression testing. We constructed additional tests to ensure that any new or changed functionality was working as intended. These developer tests included a comparison between the planetary ephemerides and JPL HORIZONS[1] and the Öpik test of gravitational focusing; both tests are described in more detail in ref. [3]. Then, a computer programmer was contracted to develop a graphical user interface (GUI), which was then verified against requirements by MEO.

As the product neared completion, we conducted several rounds of user testing. First, an internal team of testers performed coordinated sets of tests; second, external users were invited to beta test the code. Beta testing revealed a number of small errors and one more significant error in the calculation of standard deviation values, all of which were corrected before release. Shortly after release, users discovered that MEM returned non-zero meteoroid fluxes for locations inside the Moon; this was corrected in point release 3.0.1.

The above tests revealed computational errors in the code, but are not capable of testing whether the model itself is a good description of the meteoroid environment. Thus, we conducted a separate set of tests in which we compared predictions from the model with observations. In [3], we used three data sets to validate MEM 3. First, we compared the meteoroid flux at the top of the atmosphere with that measured by the Canadian Meteor Orbit Radar (CMOR; [17, 18]); we found that it matched the data quite closely. We also used MEM 3 to simulate meteoroid impact data collected by the Pegasus satellites [19] and by the Long Duration Exposure Facility (LDEF) [20].

[1] https://ssd.jpl.nasa.gov/?horizons

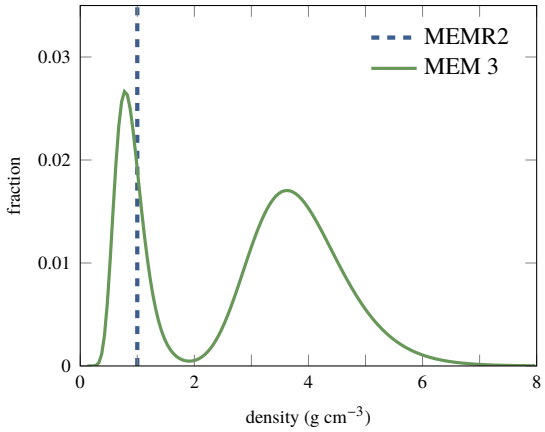

Fig. 5: Density distribution of meteoroids entering the Earth's atmosphere as calculated by MEMR2 and MEM 3.

In order to compare our MEM 3 runs with the *in situ* data from Pegasus and LDEF, we applied several sets of damage equations to the data to convert meteoroid flux information to either penetration rate or crater counts: the modified Cour-Palais damage equation [4] and the Watts and Atkinson damage equations [21]. Our analysis indicated that both sets of data include impacts from meteoroids smaller than MEM's mass range; we applied two different mass extrapolation methods to explore the range of uncertainty associated with this. Figure 6 shows the results from our simulations. In both cases, the predicted impact rate varies as we change the damage equation and mass extrapolation method. Overall, MEM 3 underpredicts the number of impacts on Pegasus and overpredicts the number of craters on LDEF. Thus, our model appears to predict a damage rate that lies between these observations.

Figure 6 also displays equivalent results obtained using MEMR2. The damage predictions from MEMR2 are in most cases lower, which is consistent with our expectation that the higher speeds and densities in MEM 3 will tend to increase predictions of damage and estimates of risk. While MEMR2 is a better match to the LDEF crater data (when the Cour-Palais damage equation is used), it falls further short of the Pegasus penetration rate. Considering both data sets together, it appears that MEMR2 may underpredict risk and damage. For this reason and because there are known errors in MEMR2, we recommend that users adopt MEM 3 for future risk assessments.

4 MODEL LIMITATIONS

MEM 3 and its predecessors have a number of limitations. Perhaps the most important limitation to be aware of is MEM's mass range: MEM describes meteoroids that are between 10^{-6} g and 10 g in mass. We limit the model to particles larger than 10^{-6} g for several reasons. First, MEM was calibrated using meteors observed by CMOR, which does not detect meteoroids below this mass limit. The second reason is that below 10^{-6} g, radiative forces such as radiation pressure and Poynting-Robertson drag become significant. As a result, the directionality and speed distribution are likely to be different below 10^{-6} g, and one cannot model these particles with MEM's populations of meteoroid orbits.

For instance, the model is considered valid only at heliocentric distances that are between 0.2 and 2 au from the Sun. Spacecraft that venture closer or farther from the Sun than these limits must use another model; a custom modeling effort may be needed. MEM also makes several approximations that assume that the user's spacecraft trajectory lies close to the ecliptic plane. So long as the spacecraft is within about 5° of the ecliptic plane, MEM 3 will be valid. Note that the inclination of an Earth-orbiting spacecraft need not be low; instead, the spacecraft in near-Earth space should be within 1.3×10^7 km of the ecliptic plane. Similarly, a spacecraft near MEM's inner boundary of 0.2 au should be within 2.6×10^7 km of the ecliptic, and a spacecraft near the 2-au outer boundary should be within 2.6×10^8 km of the ecliptic. A diagram illustrating the region of validity is shown in Fig. 7.

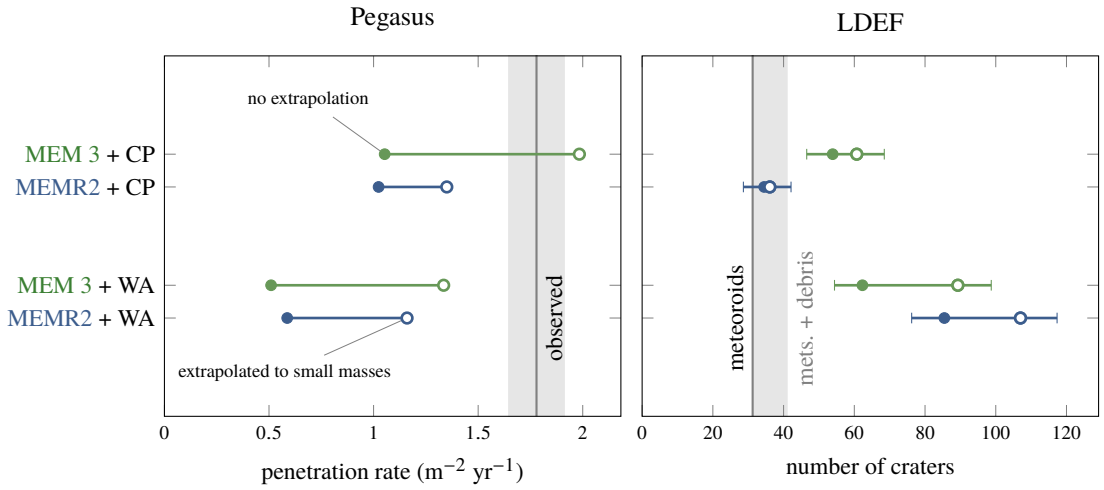

Fig. 6: A comparison between MEMR2 and MEM 3 and the rate of impacts detected by Pegasus (left) and LDEF (right). The observed impact rates are depicted as vertical block lines, and predictions obtained using MEM 3 and MEMR2 appear as green and blue points, respectively. Two damage equations (CP and WA) and two mass extrapolation approaches are included.

4 CONCLUSIONS

MEM 3 is the latest version of NASA's Meteoroid Engineering Model. It models the meteoroid environment seen by a spacecraft in the inner solar system and generates a full description of that environment that can be used in conjunction with risk assessment tools.

MEM 3 corrects several errors that exist in previous versions of the code; the most significant of these are an erroneous exaggeration in the meteoroid flux enhancement near a massive body and the erasure of correlations between meteoroid speeds and directions. Besides correcting these issues, MEM also offers meteoroid source strengths that more closely match observations at the top of the Earth's atmosphere, and a new density distribution based on meteoroid ablation modeling.

Users are likely to find MEM 3 much more convenient to use than earlier versions of the code. MEM 3 offers greater flexibility in run options, will in most cases have significantly shortened run times, avoids run-time errors present in previous releases, and warns the user of possible problems. MEM 3 can analyze transfer trajectories in a single run and provides local environments for spacecraft orbiting Mercury, Venus, and Mars as well as those near the Earth, Moon, and in interplanetary space.

Most users will obtain higher meteoroid-related risk estimates using MEM 3 than using MEMR2. MEM 3 has a higher interplanetary flux, a faster speed distribution, and a new population of dense meteoroids that will more readily puncture spacecraft. However, when we tested the code against meteoroid impact measurements from the Pegasus satellites and the Long Duration Exposure Facility, we found that MEM 3 predicted damage rates that lie between these two data sets. Thus, the higher rate of meteoroid-induced damage predicted by MEM 3 appears to be an accurate description of the environment.

5 REFERENCES

1. Cooke, W., Matney, M., Moorhead, A. V. & Vavrin, A. A comparison of damaging meteoroid and orbital debris fluxes in Earth orbit. 7TH EUROPEAN CONFERENCE ON SPACE DEBRIS, 5 pp., 2017.
2. McNamara, H. *et al.* Meteoroid Engineering Model (MEM): A Meteoroid Model For The Inner Solar System. EARTH, MOON, AND PLANETS, Vol. 95, pp. 123–139, 2004.
3. Moorhead, A. V., Kingery, A. & Ehlert, S. NASA'S Meteoroid Engineering Model (MEM) 3 and its ability to replicate spacecraft impact rates. JOURNAL OF SPACECRAFT AND ROCKETS, accepted.

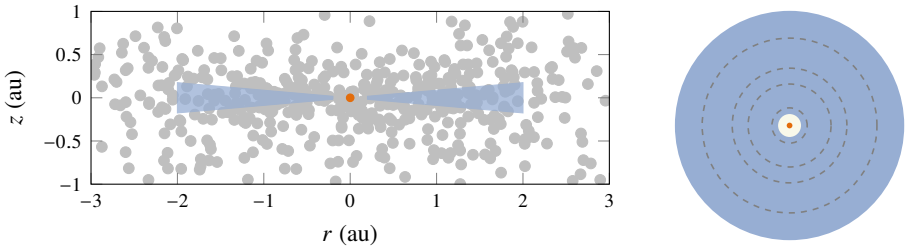

Fig. 7: The region in the inner Solar System (blue) within which MEM 3 is valid. At left we show a vertical slice through this region; the gray dots show possible meteoroid locations at a given instant in time, and the orange dot represents the Sun. At right, we show a top view of the region; here, the gray dashed circles represent the orbits of the four inner Solar System planets.

4. Hayashida, K. B. & Robinson, J. H. Single wall penetration equations. NASA-TM-103565, December 1991.
5. Jones, J. Meteoroid Engineering Model – Final Report. NASA SEE/CR-2004-400, June 2004.
6. Grun, E., Zook, H. A., Fechtig, H. & Giese, R. H. Collisional balance of the meteoritic complex. ICARUS, Vol. 62, pp. 244–272, 1985.
7. Kikwaya, J.-B., Campbell-Brown, M. & Brown, P. G. Bulk density of small meteoroids. ASTRONOMY & ASTROPHYSICS, Vol. 530, A113, 17 pp., 2011.
8. Moorhead, A. V. *et al.* A two-population sporadic meteoroid bulk density distribution and its implications for environment models. MONTHLY NOTICES OF THE ROYAL ASTRONOMICAL SOCIETY, Vol. 472, pp. 3833–3841, 2017.
9. Robertson, H. P. Dynamical effects of radiation in the solar system. MONTHLY NOTICES OF THE ROYAL ASTRONOMICAL SOCIETY, Vol. 97, pp. 423–437, 1937.
10. Burns, J. A., Lamy, P. L. & Soter, S. Radiation forces on small particles in the solar system. ICARUS, Vol. 40, pp. 1–48, 1979.
11. Kessler, D. J. A guide to using meteoroid-environment models for experiment and spacecraft design applications. NASA TN D-6596, March 1972.
12. Staubach, P., Grün, E. & Jehn, R. The meteoroid environment near earth. ADVANCES IN SPACE RESEARCH, Vol. 19, pp. 301–308, 1997.
13. Jones, J. & Poole, L. M. G. Gravitational focusing and shielding of meteoroid streams. MONTHLY NOTICES OF THE ROYAL ASTRONOMICAL SOCIETY, Vol. 375, pp. 925–930, 2007.
14. Campbell-Brown, M. D. High resolution radiant distribution and orbits of sporadic radar meteoroids. ICARUS, Vol. 196, pp. 144–163, 2008.
15. Brown, P. & Jones, J. A Determination of the Strengths of the Sporadic Radio-Meteor Sources. EARTH, MOON, AND PLANETS, Vol. 68, pp. 223–245, 1995.
16. Suggs, R. M. *et al.* Meteor properties database – final report. NASA SEE/TP-2004-400, August 2004.
17. Jones, J. *et al.* The Canadian Meteor Orbit Radar: system overview and preliminary results. PLANETARY AND SPACE SCIENCE, Vol. 53, pp. 413–421, 2005.
18. Campbell-Brown, M. D. & Jones, J. Annual variation of sporadic radar meteor rates. MONTHLY NOTICES OF THE ROYAL ASTRONOMICAL SOCIETY, Vol. 367, pp. 709–716, 2006.
19. Clifton, S. & Naumann, R. J. Pegasus satellite measurements of meteoroid penetration (Feb. 16 - Dec. 31, 1965). NASA TM X-1316, December 1966.
20. Humes, D. H. Small craters on the meteoroid and space debris impact experiment. in *LDEF: 69 Months in Space. Third Post-Retrieval Symposium*, pp. 287–322, 1995.
21. Watts, A. J. & Atkinson, D. R. Dimensional scaling for impact cratering and perforation. in *LDEF: 69 Months in Space. Third Post-Retrieval Symposium*, pp. 523–535, 1995.